Int. J. Electrochem. Sci., 16 **(2021)** 150917, doi: 10.20964/2021.01.25

International Journal of
ELECTROCHEMICAL
SCIENCE
www.electrochemsci.org

Preparation and Electrochemical Properties of $NiCo_2O_4$/rGO Composites

Changjuan Yao, Yu Su[*]*, Ying Li, Jun Li*

School of Materials Engineering, Shanghai University of Engineering Science, Shanghai, 201620, China.
[*]E-mail: suyu@sues.edu.cn

Received: 7 September 2020 / *Accepted:* 5 November 2020 / *Published:* 30 November 2020

$NiCo_2O_4$/rGO as electrode materials for supercapacitor were prepared by a facile hydrothermal route and co-precipitation. XRD and SEM were used to determine the lattice characteristics and morphology of NiCo2O4/rGO nanocomposite. It was found that GO had a good lamellar layer structure, and the overall structure was a flower-like structure. $NiCo_2O_4$ in the two methods is uniformly attached to the surface of rGO. The shape of $NiCo_2O_4$/rGO nanocomposites prepared by solvothermal method (S-NiCo) after composite is similar to that of sea urchin, and the gap distribution between needles is reasonable. The $NiCo_2O_4$/rGO nanocomposites prepared by coprecipitation method (C-NiCo) have three-dimensional network structure, and the nanocomposites are oriented. Using calomel electrode as reference electrode, a three electrode system was constructed for electrochemical experiments. The specific capacitance of $NiCo_2O_4$/rGO prepared by coprecipitation method is 1063.5F/g, that of $NiCo_2O_4$/rGO prepared by solvothermal method is 935.6F·g^{-1}, and that of NiCo2O4 prepared by coprecipitation method is 913.4F·g^{-1} by constant current charge discharge test at 2A·g^{-1}. The resistance measured by the AC impedance experiment is 1.13Ω, which is less than 1.35Ωof $NiCo_2O_4$/rGO electrode material prepared by solvothermal method.

Keywords: electrochemical, nanomaterials, supercapacitor, $NiCo_2O_4$/rGO material

1. INTRODUCTION

Supercapacitor is a new type of energy storage device with fast charge and discharge characteristics and energy storage characteristics, which energy storage capacity is between traditional capacitor and rechargeable batter. It has the advantages of high power density, short charging time, long cycle life, and environmental protection [1]. These excellent properties determine the future application of ultracapacitor in electronics, aviation, aerospace, automobile and national defense[2]. The general formula of nano spinel structure is AB_2O_4. It has excellent electrical conductivity, low loss, good chemical stability and excellent dielectric properties. The O^{2-} in the spinel structure (Fig.1) is stacked

in dense rows, in which there are $8A^{2-}$ ions, 16 B^{3+} ions, 32 O^{2-} ions. It is due to this special spatial structure that AB_2O_4 has better electrical conductivity and electrochemical activity than single metal oxide. Therefore, AB_2O_4 spinel structure has broad application prospects in the field of superconducting and lithium ion batteries as electrode materials and photocatalysis [3-6].Compared with other inexpensive metal oxides such as NiO, MnO_2, Co_3O_4 has better conductivity [7-9]. Because of the GO skeleton structure [10], the layered two-dimensional material is subjected to the buffering effect of the stress during the deintercalation process, thus the cycle stability of electrode materials can be improved. Feng [11] et al. prepared $NiCo_2O_4$/GH/NF by solvothermal method, the maximum energy density and power density are 65wh·kg^{-1} and wh·kg^{-1}, respectively, and the capacitance retention rate is 92% after 5000 cycles. Yan [12] et al. synthesized $MnSiO_3$/GO composite by simple precipitation method. Its specific capacitance at A·g^{-1} was 262.5F·g^{-1}. Paravannoora[13] et al. using magnetic nanoparticles KOH as electrolyte, nickel foam as support for embedding three-dimensional graphene hydrogel to synthesize MoS_2-G as electrode material, the specific capacitance of the electrode is 1556F·g^{-1}, and the capacitance retention rate is 94% after 5000 charge and discharge tests. Wu et al.[14] prepared the $NiCo_2O_4$ material by hydrothermal method, the specific capacitance of discharge is 983.5F·g^{-1} when the current density is 1A·g^{-1}, and the efficiency of Kulun is kept at 98.5%. Zhou [15] compounded the needle like $NiCo_2O_4$ of the vegetation–with carbon nanotubes by hydrothermal method, which contact area between the composite and the electrolyte increases, and then the ion transmission distance is shortened. At the same time, the larger internal space provides the volume change and the aggregation tendency of small particles in the cyclic process, and the composite exhibits excellent reversible properties. Therefore, rGO has good synergy with $NiCo_2O_4$. The composite $NiCo_2O_4$/rGO has good mechanical and electrochemical properties as electrode material. In this paper, $NiCo_2O_4$/rGO composites were prepared by two methods: solvothermal and coprecipitation. $NiCo_2O_4$/rGO prepared by solvothermal and co-precipitation method are marked as S-NiCo and C-NiCo.

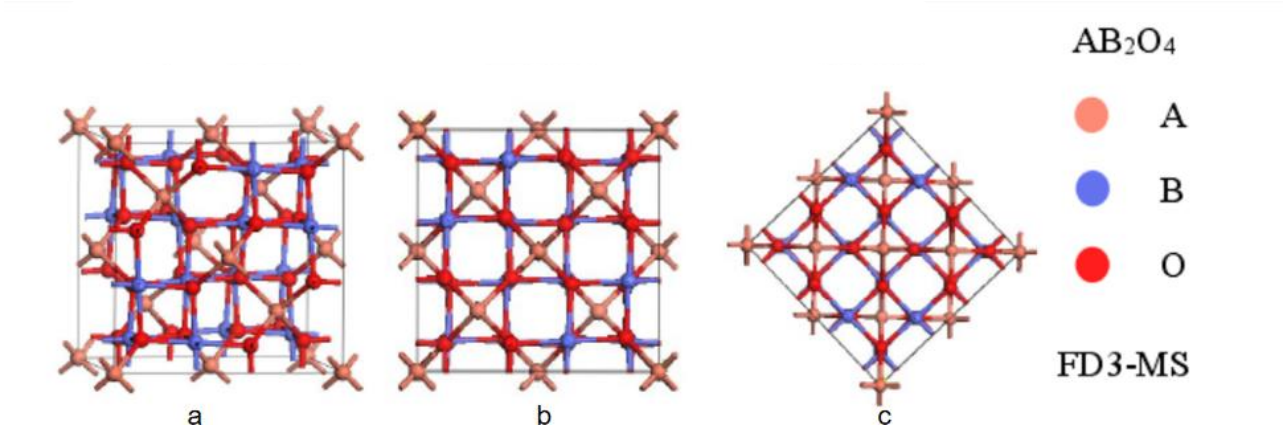

Figure 1. Schematic diagram of spinel cell (a.3D diagram, b. view, c. top view)

2. EXPERMENTAL

Except for Teflon (Daikin, Japan) and foamed nickel (Xianfeng nanonanometers), other drugs are mainly from the National Medicine Group Chemical Reagent Co., Ltd.

Electrochemical workstation was used for Autolabpgstat302 electrochemical test, the response voltage of this device is 30V, the maximum current is 2A. According to the peak current Lp of CV Curve, the relationship between response current and potential is obtained

$$C_m = \frac{\int idv}{v \cdot msv}$$

Cm is the specific capacitance of the electrode, F·g-1. v is the scanning rate of the experiment, v·s-1;m is the mass of the active substance ,g; δv is discharge voltage drop, v.

2.1. Preparation of GO

The preparation process of GO can be divided into five stages. The stages are mainly divided into low, medium, and high temperature reaction stages, treatment stage and separation stage because of different reaction temperature.

（1）Low temperature reaction stage (4-20℃): dissolve graphite powder into beaker, add concentrated sulfuric acid and concentrated phosphoric acid mixture in ice water bath, stir for 0.5h , add Potassium Permanganate and continue stirring for 2h. This process should be controled under 20℃.

（2）Medium temperature reaction stage (35-80℃): remove ice water bath, heat up to 35℃, continue stirring for 30min and slowly add 100mL deionized water. this process will continue to be no less than 2h. The main purpose of meso temperature reaction is deep oxidation of graphite.

（3）High temperature reaction stage (98℃): water heating control temperature is 98℃, stirring for 30min –continuously, the solution is changed from reddish brown to golden yellow. The reaction process is mainly the hydrolysis reaction of interlayer compounds, dissociating graphite oxide and removing sulfur containing group.

（4）Treatment phase: cooling slowly, keep the solution temperature at 40-50℃, and add 30% H_2O_2 solution to neutralize the remaining oxidants in the above reaction process until no bubbles are generated.

（5）Separation stage: add sufficient amount of dilute HCl to the beaker, rest for 10h, pour the upper clear liquid, shake with proper amount of deionized water, centrifuge and precipitate until the pH value is neutral. Put it in the surface pan, and dry it at 80℃, and get the GO powder. The action of this step is to adjust the PH of GO as neutral and wash out the impurity ions.

2.2 Preparation of NiCo2O4 single material

$NiCo_2O_4$ materials prepared by solvothermal method can get high purity products. The specific preparation steps are as follows:

（1）The precursor solution was prepared by electronic balance, called 10mmol, pure $Co(NO_3)_2 \cdot 6H_20$, 5mmol pure $n(Co^{2+}):n(Ni^{2+})=2:1$ the addition of deionized water and sulfur into the beaker, covered with plastic wrap, and stirring with electromagnetic stirrer for 30min, adding slowly the pure urea and stirring for 30min. A transparent solution of deep pink is obtained, providing nickel and cobalt sources for subsequent reactions.

（2）$NiCo_2O_4$ was prepared: pour the solution into the reactor and heat up to 120℃ for 12h. After the reactor was removed, the product was reduced to room temperature. The product was green, washed repeatedly with a small amount of deionized water and absolute alcohol, centrifugally precipitated, placed in a surface dish, and dried at 60℃, and obtained precursor powder of $NiCo_2O_4$ material.Calcined in air for 2h at 300℃(heating rate of 1℃·min^{-1}), black powder products were obtained. The reaction equation for calcination is as follows:

$$2NiCo(OH)_x(CO3)_y \square nH2O+O_2 \rightarrow 2NiCo_2O_4+(x+2n)H_2O+2yCO_2$$

2.3 Preparation of NiCo2O4/rGO composite

Method 1: $NiCo_2O_4$/rGO composite was prepared by solvothermal method.

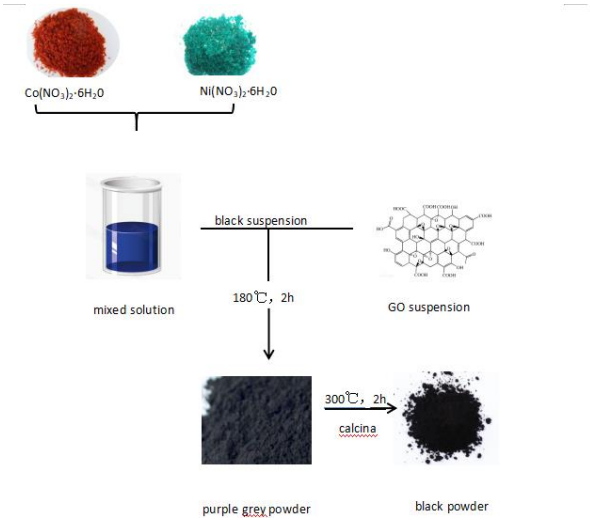

Figure 2. The chart of the solvothermal method (the mixture of liquid and GO suspension is replaced by functional group or molecular formula).

（1）0.2g GO powder was dispersed in 100mL deionized water to obtain stable GO suspension. 0.8mmol analytical pure $Co(NO_3)_2·6H_20$ was obtained, and the pure analytical 0.4mmol was dissolved in the deionized water, and the reaction was fully stirred for 15min.

（2）Under the condition of ultrasonic vibration, the $Co(NO_3)_2·6H_20$and $Ni(NO_3)_2·6H_20$mixed solution were added slowly into the GO suspension by the rubber head dropper, and the ultrasound was subjected to ultrasonic for 30 min.

（3）The mixed solution was reacted at 180℃ for 2h(heating rate was 1℃·min^{-1}). The reactor was cooled to room temperature, and the product was washed repeatedly with absolute alcohol and deionized water, precipitated centrifugally and dried at 60℃.

（4）The dried powder was calcined at 300℃ for 2h, and the black $NiCo_2O_4$/rGO composite material was obtained from.

Method 2: $NiCo_2O_4$/rGO composite material was prepared by coprecipitation method.

(1) A certain amount of rGO is dissolved in deionized water to obtain 1mg·mL^{-1} solution.

(2) A certain amount of $NiCo_2O_4$ powder was dispersed in deionized water. After ultrasonic dispersion, the rGO suspension was mixed with the above solution and dispersed by ultrasonic to make the two materials fully mixed.

(3) The products obtained by filtration of mixed solutions were washed with absolute alcohol and deionized water for several times, and dried at 54℃ for 24h.

(4) The black $NiCo_2O_4$/rGO composite was obtained by calcining the dried powder at 300℃ for 2h.

In the experiment, the lattice characteristics of the material were tested by PANalytical X`Per PRO X ray diffractometer (XRD), and the surface topography of the material was observed by S-3400N scanning electron microscope (SEM) of Hitachi. The three electrode test used the HZC-002 type equipment of Hangzhou SEO electrochemical test equipment Co., Ltd. The electrochemical performance of samples were tested by the Wantong company AUTOLAB PGSTAT302 electrochemical workstation .

2.4. Electrochemical measurement

The as-prepared three-electrode system was placed in a 1 M KOH aqueous solution, which included a working electrode, counter electrode (Pt) and reference electrode (Hg/HgO), and the electrochemical measurement was carried out on an electrochemical workstation (HZC-002). The working electrodes were fabricated by combining the active material ($NiCo_2O_4$ or $NiCo_2O_4$/rGO), SUPER P Li and PTFE. The slurry was pasted onto the Ni foam, pressed at 10 MPa and dried at 60 °C overnight. The mass loading of the $NiCo_2O_4$ and $NiCo_2O_4$/rGO was 5 mg. Cyclic voltammetry (CV) measurements were performed at different scan rates from 5 to100 mV·s−1. Galvanostatic charge-discharge (GCD) tests were conducted at current densities from 2 to 10.0 A·g^{-1}. Electrochemical impedance spectroscopy (EIS) characteristics were tested with a frequency of 0.01–100 KHz.

3. RESULTS AND DISCUSSION

Comparing with the reference card (JCPDS 20-0781) of $NiCo_2O_4$ material, it is found that the XRD data coincide with the data on the reference card, indicating that $NiCo_2O_4$ material has been successfully synthesized. After comparing the composite and reference materials, the diffraction peaks at 18.9° and 31.2° have been weakened. Because of the addition of graphene, the crystallization properties of $NiCo_2O_4$ decreased .

From Fig.3b, the GO prepared by the modified Hummers method exhibits a 3D flower-like structure, and the graphene oxide particles are uniform in size, and no obvious agglomeration occurs. The thickness of the prepared GO sheet is about 15 μm , there are obvious wrinkles on the surface, and a layered graphene layer can be observed. The thickness of the sheet layer is about 0.5 μm , the hole spacing is about 2.5 μm , and the hole depth is about It is 3 μm .

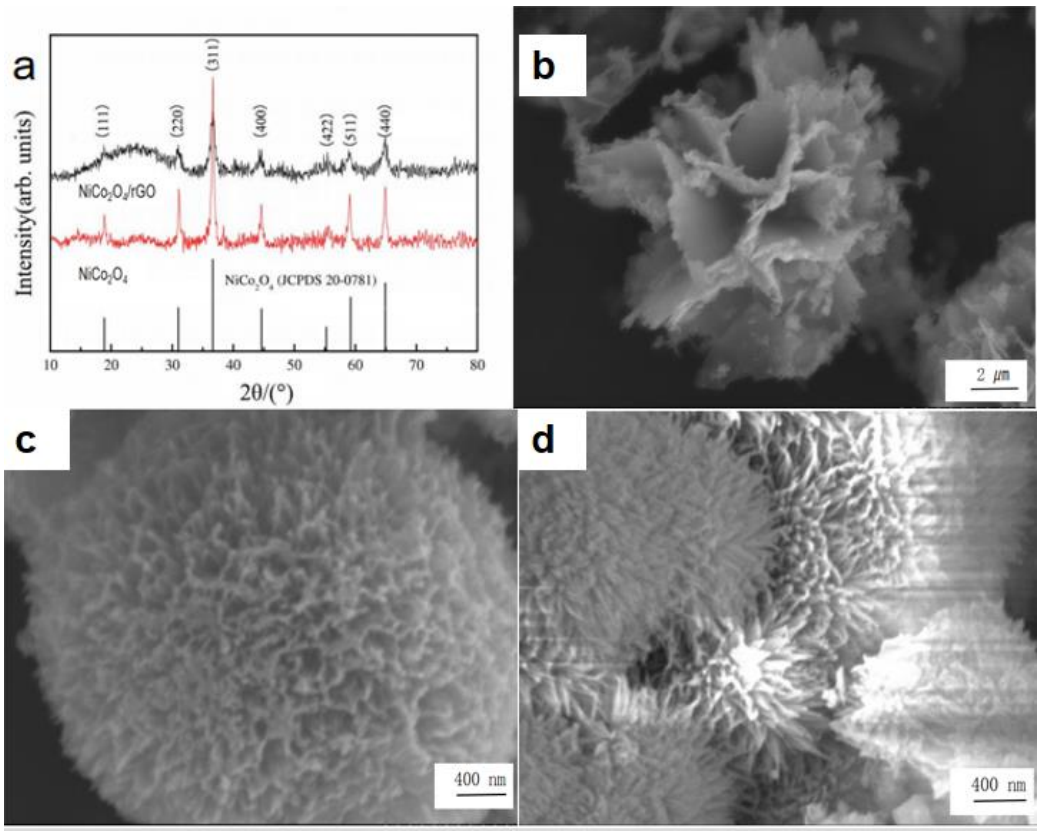

Figure 3. (a)X ray diffractometer patterns of $NiCo_2O_4$/rGO and $NiCo_2O_4$;(b) Scanning electron microscope of GO ; (c)Scanning electron microscope images of C-NiCo (co-precipitation); (d)Scanning electron microscope S-NiCo (solvothermal).

It can be seen from Fig.3c that C-NiCo exhibits a porous three-dimensional spherical shape, $NiCo_2O_4$ is attached uniformly to the surface of rGO, and $NiCo_2O_4$ is nano-sheet-shaped protrusions and intermingled . And the array of nano-sheets arranged neatly constitutes a large amount of open space. The formed three-dimensional network structure is conducive to the transport of electrolyte ions and electrons, and increases the active site of electrode reactions and the stability of electrochemistry.

In Fig.3d, the nanowire-shaped $NiCo_2O_4$ material is uniformly attached to the surface of rGO through compounding, showing a hairball shape. RGO serves as a growth substrate for the $NiCo_2O_4$ material and is covered by the nanowire-shaped $NiCo_2O_4$. In addition, there is a clear gap between the needles and the needles grow directionally. The $NiCo_2O_4$ not only has excellent mechanical properties by the way of in-situ growth, but it is not easy to fall off during the process of charging and discharging. $NiCo_2O_4$ /rGO facilitates the diffusion of ions in the gaps. In the composite mode of rGO and $NiCo_2O_4$, rGO mainly plays a supporting and conductive role, and the $NiCo_2O_4$ spinel structure shows the performance of pseudocapacitance [16]. The needles of S-NiCo are evenly distributed, and the gap is more moderate, the contact area with the electrolyte is large, the transmission path of ions is shortened, and the electrochemical performance of the composite material is improved.

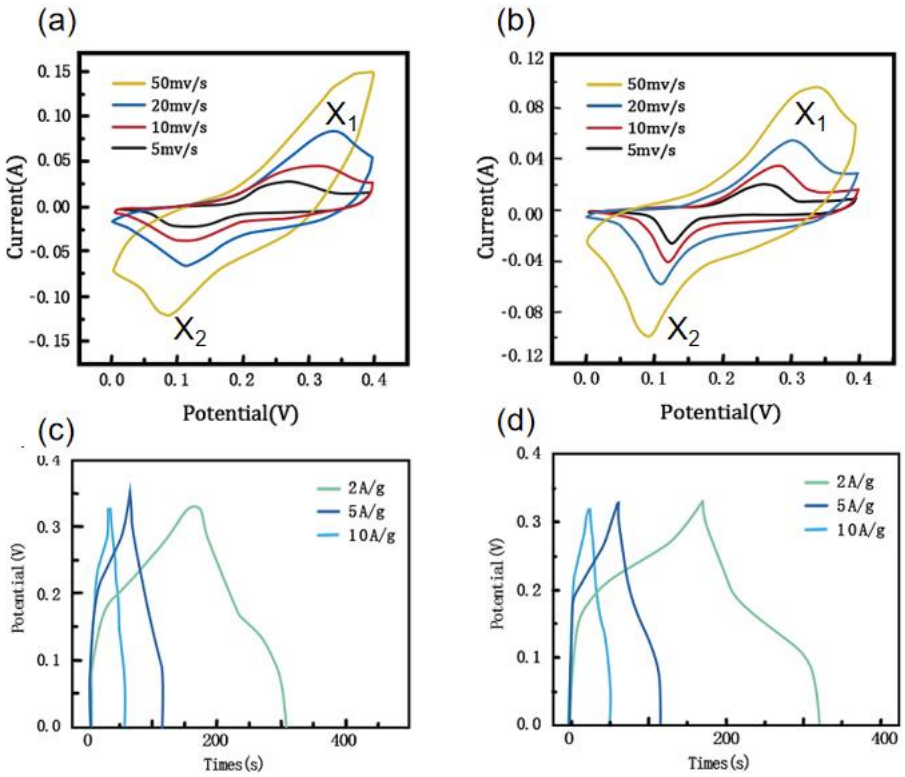

Figure 4. (a) Cycle voltammetry (CV) curves of S-NiCo at different scan rate of 5 mV/s, 10mV/s, 20mV/s, 50mV/s; (b)Cycle voltammetry CV curves of C-NiCo at different scan rate of 5 mV/s, 10mV/s, 20mV/s, 50mV/s; (c) S-NiCo electrode material charge and discharge at current densities of 2 A/g, 5A/g, 10A/g; (d) C-NiCoelectrode material charge and discharge at current densities of 2 A/g, 5A/g, 10A/g.

Fig.4a is a curve of S-NiCo at the potential window of 0-0.4V, and the scanning rates are 5mV·s^{-1}, 10mV·s^{-1}, 20mV·s^{-1} and 50mV·s^{-1} respectively. Supercapacitors are mainly used to store energy (reversible) by redox reaction. In Fig.4, there are two pairs of redox peaks in the curve prepared by solvothermal method. It might be related to the transformation of the equivalent states of Co^{2+}/Co^{3+}/Co^{4+} and Ni^{2+}/Ni $^{3+}$/Ni^{4+}, indicating that the existence of pseudo capacitance is the main mechanism of the storage of electricity.

Fig.4b shows the CV curve of C-NiCo at different scanning rates. It can be seen that the CV curve has no obvious deformation–with the increase of scanning rate.It is shown that $NiCo_2O_4$/rGO material has good chemical stability, reversibility and small equivalent series resistance (ESR). At the same time, the sealing area of C-NiCo electrode is larger than that of S-NiCo electrode. According to the formula, the specific capacitance of $NiCo_2O_4$/rGO electrode at different scanning rates can be obtained from the closed area of CV curve. At the same scanning rate, the larger the sealing area of CV curve, the larger the specific capacitance of the material. The results show that the C-NiCo electrode material has higher specific capacitance. Compared with 4a-b, we found that the $NiCo_2O_4$/rGO nanocomposite electrode materials both had two pairs of redox peaks. On the left side of the redox peak, we call EDL region. We can see from the CV curve that the double layer capacitance is very small due

to the adsorption of electric particles at the interface be very small, so no redox reaction occurs here. The irreversible hydrogen evolution reaction on the right side of the redox peak (OER).

According to the references [17] , the redox reaction on the surface of $NiCo_2O_4$/rGO is:

$$NiCo_2O_4 + OH^- + H_2O \leftrightarrow NiOOH + CoOOH + 2e^-$$

$$CoOOH + H_2O \leftrightarrow CoO_2 + H_2O + e^-$$

Fig.4c-d Comparison of the GCD curves of the two materials shows that C-NiCo electrode prepared has the longest discharge time and the highest specific capacitance. The GCD measurement results are consistent with the CV measurement results. This indicates that the addition of rGO plays an important role in improving the performance of the electrode material, and proves that the rGO and $NiCo_2O_4$/rGO have good synergy.It not only preserves excellent electrical conductivity of rGO, but also has electrochemical stability and excellent capacitance of transition bimetallic oxide [21].

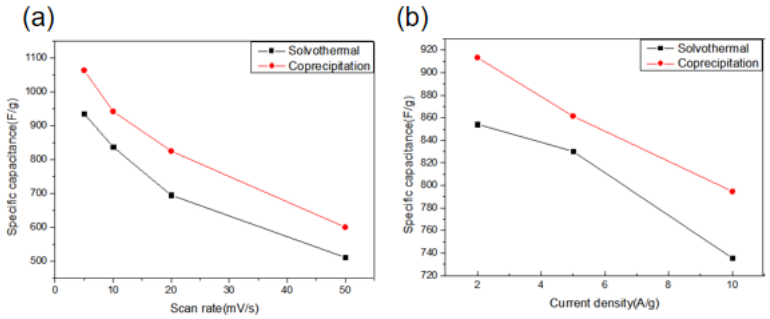

Figure 5. (a) Relationship between specific capacitance and scan rate of 5 mV/s, 10mV/s, 20mV/s, 50mV/s; (b) Relationship between specific capacitance and current density of 2 A/g, 5A/g, 10A/g.

Under the scanning rate of 5mV·s^{-1}, 10mV·s^{-1}, 20mV·s^{-1} and 50mV·s^{-1}, the CS (specific capacitance) of $NiCo_2O_4$/rGO composite-both decreased with the increase of scanning rate.The Cs of C-NiCo composite electrode prepared is much higher than that of the S-NiCo[18]. When the scanning rate reaches 50mV·s^{-1}, the capacity of C-NiCo composite electrode is still 56.4%, that of S-NiCo electrode is 54.6% . The stability is higher than that of solvothermal electrode. This is related to the porous three-dimensional spherical pore structure in $NiCo_2O_4$/rGO SEM(Fig.3c). This unique structure can provide an efficient ion transport channel, and make the composite have a very ideal rate and good cycle stability [19].Cheng and his colleagues reported a new hybrid nanostructure, rGO modified $NiCo_2O_4$ nanosheets, because the support of nickel foam does not require the use of binder. However, the uneven distribution of a structure seriously affects the electrochemical stability and ion transport of the materials [20].

Fig5b shows the change rule of specific capacitance with current density. The specific capacitance of C-NiCo is higher than that of $NiCo_2O_4$/rGO prepared by solvothermal method under different current density. The specific capacitance of C-NiCo is higher than that of S-NiCo under different current density. With the increase of current from 2A·g^{-1} to 10A·g^{-1}, the initial capacitance (913.4F·g^{-1}) of C-NiCo electrode is about 87.0%, indicating that the S-NiCo electrode has good rate performance. Meng and his team used nanomaterials prepared by hydrothermal method and spray

method. rGO is draped on $NiCo_2O_4$ and $NiCo_2O_4$ is fluffy ball. The specific capacitance of 0.5g was 702F·g^{-1}[22].Table 1 shows the comparison of the specific capacitance of the published polyaniline and carbon material electrodes and this study. It is clear that the specific capacitance of C-NiCO prepared in this study is similar or higher than those reported in other papers.

Table 1. Comparison of the specific capacitance values of $NiCo_2O_4$ materials reported in this and other works.

Materials	Supercapacitor capacitance	Morphology	Fabrication techniques	Reference
$NiCo_2O_4$	218 F/g(100 mA/g)	Flocculent particles	Coprecipitation	24
$NiCo_2O_4$	983.5F/g(1 A/g)	Nanowires	Hydrothermal	25
$NiCo_2O_4$	1068F/g(1 A/g)	Bowl-shaped	Soft template hydrothermal method	26
NiCo2O4/CB@carbon nanofiber	846F/g(1 A/g)	Nanowires	Hydrothermal	27
NiCo-MOF@PNTs	1109F/g(0.5 A/g)	Nanosheets	ultrasonic method	28
C-NiCO	913.4F/g(2 A/g)	three-dimension-al spherical shape	Coprecipitation	This work

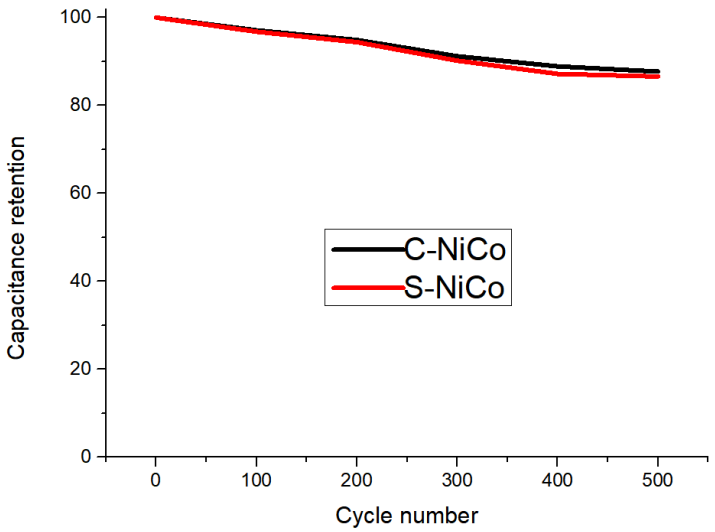

Figure 6. cycling stability performance of all the electrodes at 2 A/g/.

Fig. 6 demonstrates cyclic stability of all the electrodes. Among all the electrodes, C-NiCo showed better stability compared to other electrodes. It is noticed that when constant current density (2 A·g^{-1}) is applied for the first cycle, the value of Cs turns out to be maximum. As the number of cycle is

increased to 500, the overall capacity is decreased to only 12% of its initial value. A relatively better stability of C-NiCo electrode could be due to the interconnection of rGO sheets with $NiCo_2O_4$ to form three-dimensional spherical shape like structures, leading to the barrier free contact which minimizes the internal resistance of the electrode remarkably [23].

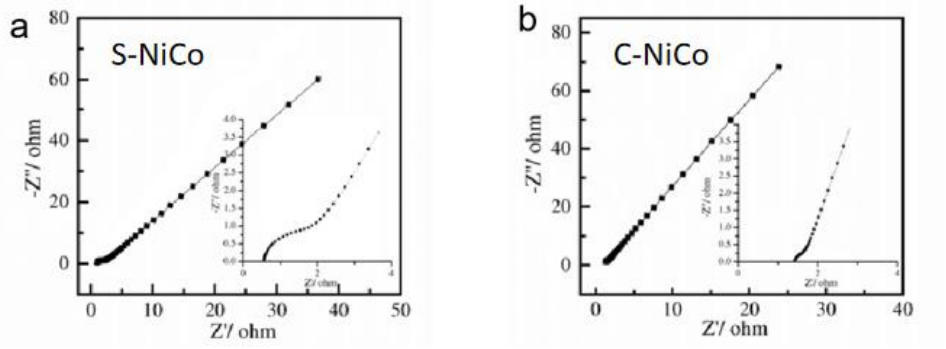

Figure 7. (a) Nyquist plots (EIS) of the S-NiCo; (b) Nyquist plots (EIS) of the C-NiCo.

In Fig.7 the AC impedance diagram of the two materials is made up of high frequency Nyquist curve and low frequency linear line. The resistance of C-NiCo is 1.13 Ω , while the resistance of S-NiCo is 1.35 Ω. On the other hand, it is proved that the electrode material contacts well with the electrolyte.The resistance of $NiCo_2O_4$/rGO material electrode prepared by the two methods is relatively small, indicating that adding GO can reduce the resistance of the composite electrode, indicating that its resistance to ion migration is relatively small.This is attributed to the more dense and uniform three-dimensional structure formed on the surface after the recombination. The C-NiCo are more reasonable in space distribution and have enough space for the ions to move between them. At the same time, the larger specific area of the composite will make the electrons move faster, and increase the active sites and reaction rates of the reaction. However, the C-NiCo shows a relatively low resistance.

The aim of this study is to explore a new efficient, convenient and inexpensive synthetic electrode material. The two methods of preparation are compared. The C-NiCo composite has excellent electrochemical properties. Subsequent studies can use the first principles to calculate the interactions between different atomic orbitals in different preparation processes and generate transition products. And the growth rate of different planes of $NiCo_2O_4$ is calculated, and the growth regularity and morphologies evolution rule of each crystal surface are clarified.

4. CONCLUSIONS

The combination of $NiCo_2O_4$ and rGO materials has increased the electrochemical performance of the composites without controversy. Compared with the S-NiCo and C-NiCo, it is concluded that:

(1) in structure, the specific surface area of the composite prepared by the two methods is increased, which is conducive to the movement of ions between the gaps and has good electrical conductivity.

(2) the electrochemical performance shows that the specific capacitance of the $NiCo_2O_4$/rGO

electrode prepared by coprecipitation method is 1063.5F·g^{-1} by the CV curve. The experimental results of galvanostatic charging and discharging show that the specific capacitance of the electrode prepared by the coprecipitation method is 5mV/s. On the other hand, the resistance of C-NiCo electrode is only 1.13Ω. As the number of cycle is increased to 500, the overall capacity is decreased to only 12% of its initial value. $NiCo_2O_4$/rGO prepared by either method, low resistance, more efficient charge and discharge platform, and better Faraday redox reaction. $NiCo_2O_4$/rGO electrode material's energy storage mechanism is redox reaction, depending on the change of ionic valence state to store energy. Both composites exhibited the good electrochemical properties.

References

1. D. Li, Y. L.Liu B. P. Lin, *Prog. Chem.*, 27(2015) 404.
2. M. M. Liu , C. Cai, Z. J. Zhang R. LIU, *Mater. Rep*., 33(2019) 103.
3. J. Fu, C. J. Desantis, R. G. Weiner, S. E. Skrabalak. *Chem. Mater.*, 27(2015) 1863.
4. Q. Zhou, B. Zheng, Z. Y. Li, Y. F. Wang, *Chin. J. Inorg. Chem.*, 33(2017) 1416.
5. F. X. Ma, L. Yu, C, Y. Xu, X. W. Lou, *Energy Environ. Sci*., 9(2016) 862.
6. G. Liu, J. Shao, Y. J. Gao, Q. Qu, *Chinese. J. Chem.*, 35(2017) 67.
7. J. J. Chen, Y. Huang, H. Y. Huang, *Dev. Appl. Mater*., 30(2015) 90.
8. X. C. Dong, C. Su, W. J. Zhang, C. Ge, L. Zhao, X. J. Wang, H. Y. Zhang, J. Chen, Z. M. Wang, L. T. Sun, J *Mater. Sci. Technol.*, 33(2017) 793.
9. H. Y. Wu, H. W. Wang, *Acta. Phys-Chim. Sin.*, 29(2013) 1501.
10. B. Hu, H. P. Zhang, L. L. Jiang, *Acta. Mater. Compos. Sin.*,35(2018) 661.
11. H. F. Feng, S. Y. Gao, S. Jun, L. Zhang, Z. M. Peng, S. K. Gao, *Electrochimica. Acta*, 299(2019) 116.
12. Cheng Y, Zhang Y, Wang Q, C. Meng, *Colloid Srface* A, 562(2019) 93.
13. A. Paravannoor, A. Baidu, *Surf. Interf.*, 14(2019) 256.
14. J. Z. Wu, D. D. Lu, R. Zhang,Y. R. Zhu, S. Y. Yang, R. S. Zhu, Y. F. Yi, *Mod. Chem. Ind.*, 36(2016) 80.
15. G. Zhou, C. Wu, Y. H. Wei, C. Z. Li, Q. W. Lian, C. Cui, W. F. Wei, L. B. Chen, *Electrochimica. Acta*, 222(2016) 1878.
16. W. S. Wei, Z. X. Song, W. Zeng, *Mater. Sci. Technol*., 26(2018) 47.
17. X. Li, *China. Electronic. Market*., 11(2009) 52.
18. E. Mitchell, A. Jimenez, R. K. Gupta, *New. J. Chem.,* 39(2015) 2181.
19. V. Venkatachalam1, A. Alsalme, A. Alghamdi, *Ionics*., 23(2017) 977.
20. Z.B. Wu, Y.R. Zhua, X.B. *J. Phys. Chem. A,* 36(2014) 14759.
21. S. M. Li, Y. Kang, P. W. Ye, K. R. Ma, Z. Zhang, Q. Huang, *Appl. Surf. Sci*., 503(2020) 144090.
22. S. Ramesh, D. Vikraman, H.S. Kim, H.S. Kim, J.H. Kim, *J. Alloys Compd*., 765(2018) 369.
23. F. B. Meng, L. C. Zhao, Y. Y. Zhang, J. Zhai, Y. J. Li, W. Zhang, *Ceram. Int.*, 45(2019) 23701.
24. Y. Zhang, S. W. Wang, H. L. Gao, S. Q. Zhao, *CJPS*, 42(2018) 212.
25. W.D. Qiu, H.B. Xiao, M.H. Yu, *Chem. Eng.J*., 352(2018) 996.
26. R. Y. Liu, H. R. Wu, Z. Wang, H. Wei, Y. Y. Mai, *Sci. China Mater*.,19(2020) 1.
27. K. Peng, C. Mang, Z. W. Liu, Z. Q. Ai, Q. Q. Li, J. L. Shi, Y. Song,*Carbon Techniq.*, 39(2020) 9.
28. Y. X. Liu, Y. Z. Wang,Y. J. Chen,C. Wang, L. Guo, *Appl. Surf. Sci.*,507(2020) 145089.